Carbohydrate Polymers 117 (2015) 853–861

Contents lists available at ScienceDirect

Carbohydrate Polymers

journal homepage: www.elsevier.com/locate/carbpol

Physicochemical properties of complex rhamnogalacturonan I from gelatinous cell walls of flax fibers

Polina V. Mikshina[a], Bulat Z. Idiyatullin[a], Anna A. Petrova[a], Alexander S. Shashkov[b], Yuriy F. Zuev[a], Tatyana A. Gorshkova[a,*]

[a] Kazan Institute of Biochemistry and Biophysics, Kazan Scientific Center, Russian Academy of Sciences, Lobachevsky Str. 2/31, P.O. Box 30, 420111 Kazan, Russia
[b] Zelinsky Institute of Organic Chemistry, Russian Academy of Sciences, Leninsky Pr., 47, 119991 Moscow, Russia

ARTICLE INFO

Article history:
Received 1 July 2014
Received in revised form
29 September 2014
Accepted 11 October 2014
Available online 24 October 2014

Keywords:
Flax fibers
Plant polysaccharides
Rhamnogalacturonan I
Self-diffusion
Aggregation

ABSTRACT

The physicochemical properties of flax fiber cell wall rhamnogalacturonan I (RG-I) and its fragments, obtained after galactanase treatment (fraction G1), were characterized. RG-I retains its hydrodynamic volume after its molecular weight decreases by approximately half, as revealed by SEC. Two techniques, DLS and NMR, with different principles of diffusion experiment were used to establish the reasons for this property of RG-I. Three possible types of particles were revealed by DLS depending on the concentration of the RG-I and G1 solutions (2–2.5, 15–20, and 150–200 nm). It was determined by BPP-LED experiments that the backbone of the RG-I was 1.3–1.9-fold more mobile than the side chains. The obtained data suggest a novel type of pectin spatial organization—the formation of RG-I associates with the backbone at the periphery and the interaction between the side chains to form a core zone.

1. Introduction

Among the most complex plant cell wall polymers is the large family of pectins, named rhamnogalacturonans I (RG-I). These diverse polysaccharides are joined into one group, because all of them have repeating dimers [→4)-α-D-GalpA-(1 → 2)-α-L-Rhap(1→] in their backbones. The variability of RG-I is mainly provided by the distribution and structure of the side chains, which are usually attached to the O-4 of the rhamnose residues. These side chains are made of galactose and/or arabinose and may have different properties, including lengths, degrees of branching, and types of linkages (Visser & Voragen, 1996; Ridley, O'Neill, & Mohnen, 2001; Yapo, 2011).

RGs-I are usually considered to be the components of the thin primary cell walls (McNeil, Darvill, & Albersheim, 1980; Ridley et al., 2001); however, they were detected both cytochemically (Bowling & Vaughn, 2008) and biochemically (Gurjanov, Ibragimova, Gnezdilov, & Gorshkova, 2008) within specific type of thick cell walls with high cellulose content. This type of cell wall is called the "gelatinous"; it is widely distributed among plant species, but is developed only in fibers (Gorshkova & Morvan, 2006; Gorshkova et al., 2010). Such fibers present for instance in tension wood and fiber crops are characterized by contractile properties, which have the origin in thick gelatinous layer of cell wall (Mellerowicz & Gorshkova, 2012). One of the ideas on the origin of tension within the gelatinous cell wall suggests that it is based on the lateral interaction between cellulose microfibrils, accompanied by matrix polysaccharide entrapment (Mellerowicz, Immerzeel, & Hayashi, 2008). Among the proposed matrix polysaccharides for such a role is RG-I (Gorshkova et al., 2010).

The most studied RG-I from the gelatinous cell walls is the polysaccharide from flax phloem fibers (Gorshkova & Morvan, 2006; Gurjanov et al., 2008; Mikshina et al., 2012). This polymer is fiber-specific and is formed only during the deposition of the gelatinous cell wall (Gorshkova et al., 2004). *In muro*, it is effectively retained by cellulose microfibrils so it cannot be fully extracted even by concentrated alkali; it is possible to isolate it in the polymeric form only after microfibril destruction (Gurjanov et al., 2008). Obtained in this way, RG-I elutes in the 100–400 kD region and has side chains built mainly of β-(1 → 4)-galactose. In the flax cell wall RG-I, three-fourths of the rhamnose residues are unbranched (28%) or substituted by single galactose residues (47%); oligogalactose side chains are joined to a quarter of total rhamnose, their average length is 14 monomers (Mikshina et al., 2012). It is logical to

* Corresponding author. Tel.: +7 843 292 53 32; fax: +7 843 292 73 47.
E-mail address: gorshkova@mail.knc.ru (T.A. Gorshkova).

http://dx.doi.org/10.1016/j.carbpol.2014.10.037
0144-8617/

assume that since it is a tissue-specific polymer from gelatinous cell walls with contractile properties, this polysaccharide may possess specific physicochemical parameters provided by specific spatial structure.

This study aimed to characterize the hydrodynamic properties and spatial structure of RG-I from flax fiber gelatinous cell walls. For this, we used size-exclusion chromatography (SEC), and approaches based on the determination of hydrodynamic dimensions of particles through their diffusive mobility–dynamic light scattering (DLS) and nuclear magnetic resonance spectroscopy (NMR)–to analyze RG-I and its fragments obtained after galactanase treatment. Data on the hydrodynamic behavior of complex polysaccharides, such as RG-I, are scarce; to avoid methodological artifacts, we analyzed several commercial pullulans using the same approaches and compared the parameters that we have received with those reported by other researchers for these polysaccharides. The obtained results revealed unusual hydrodynamic properties of the complex RG-I from the cell walls of flax fibers that suggest the association of individual molecules into large complexes. Within such association, the RG-I backbone is located at the surface and galactan side chains form the core zone.

2. Materials and methods

2.1. Plant material

Flax plants (*Linum usitatissimum* L. cv. Mogilevski) from the collection of the All-Russian Flax Research Institute (Torzhok, Russia) were grown in boxes, with a 50-cm soil layer, in the open air, under natural light, and with daily watering. Mature non-retted flax stems (100 days after sowing) were used for isolation of RG-I from cell wall.

2.2. Isolation of the fiber cell wall RG-I

Isolation of cell wall RG-I was performed according to the procedure developed by Gurjanov et al., 2008. The residue, remaining after cell wall sequential treatments with 1% ammonium oxalate and 4 M KOH, was dissolved in 8% LiCl in *N*,*N*-dimethylacetamide. Cellulose was precipitated by water and completely degraded by cellulase (Cellusoft-L; Novo Nordisk Bioindustrrie S.A., Paris, France; 750 EGU/G). Matrix polysaccharides, which remained in the polymeric form (molecular weight: 100–400 kD), were purified from the low molecular weight products and salts on a Sephadex G-25 column (Pharmacia, Sweden). The yield of the isolated RG-I was ~3% of the residue obtained after KOH treatment.

2.3. Pullulans

In all experiments, four pullulan samples of 1660, 380, 100, and 48 kD (Showa Denko, Japan) with low index of polydispersity (1.09–1.19) were used as standards.

2.4. Hydrolysis of RG-I by endo-β-1 → 4-galactanase

Highly purified and well characterized endo-β-1 → 4-galactanase from *Aspergillus aculeatus* (Novo Nordisk, A/S, Copenhagen, Denmark) (Van de Vis, Searle-van Leeuwen, Siliha, Kormelink, & Voragen, 1991) was kindly provided by Prof. H.A. Schols (Wageningen University, The Netherlands). To remove salts and low molecular weight substances, the enzyme was passed through a Sephadex G-25 column (Pharmacia, Sweden). Elution was performed with 0.01 M NaOAc, pH 5.0. Protein was quantified by the method described by Bradford (Bradford, 1976).

Before the polymer incubation with endo-β-1 → 4-galactanase, an additional saponification step was performed for removing methyl ester and acetyl groups according to the previously described procedure (Mikshina et al., 2012; Gur'janov, Gorshkova, Kabel, Schols, & van Dam, 2007). The treatment by the enzyme (25 μg of protein per 5 mg of substrate) was performed at 40 °C for 48 h in 0.01 M NaOAc, pH 5.0 in an IS-971R incubator shaker (Jeio Tech, Korea) at 120 rpm. The enzyme was inactivated at 100 °C for 5 min.

2.5. Size-exclusion chromatography

Size exclusion chromatography of RG-I and its fragments obtained after galactanase treatment was carried out on a Sepharose CL-4B column (1.2 × 40 cm Pharmacia, Sweden) using 0.01 M pyridine/acetic acid solution, pH 4.5, flow rate 0.25 mL min^{-1}, 1.0 mL fractions. Sugar content in each fraction was measured by phenol-sulfuric acid assay (Dubois, Gilles, & Hamilton, 1956).

For calculation of weight-average ($\bar{M}_w$) and number-average ($\bar{M}_n$) molecular weight, the chromatogram was split into slices along the retention time axis; for each slice its area A_i and molecular weight M_i (corresponding to the center of the slice) were determined. Average molecular weights were calculated by the equations:

$$\bar{M}_w = \frac{\sum_i A_i M_i}{\sum_i (A_i)}, \quad \bar{M}_n = \frac{\sum_i A_i}{\sum_i \left(A_i / M_i\right)} \tag{1}$$

2.6. Monosaccharide analysis

The samples were hydrolyzed with 2 M TFA (Sigma, USA) at 120 °C for 1 h and dried in a stream of air at 60 °C. Monosaccharide analysis was carried out by high performance anion-exchange chromatography (HPAEC) on CarboPac PA-1 column (4 × 250 mm, Dionex, USA), using pulse-amperometric detection (Dionex, USA); ED 40 waveform for the analysis of carbohydrates by ion chromatography using a gold electrode was applied. Eluents: A–0.015 M NaOH; B—1 M NaOAc in 0.1 M NaOH. The column was equilibrated with eluent A–100%. The sample was eluted with following linear gradient: 0–20 min A—100%; 20–21 min A—90%, B—10%; 21–31 min A—70%, B—30%; flow rate 1 mL min^{-1} at 30 °C. Monosaccharide standards were treated with 2 M TFA at 120 °C, 1 h before they were used for calibration.

2.7. Dynamic light scattering

The samples of RG-I and pullulans were dissolved in MilliQ water, centrifuged at 12,000 × *g* for 10 min and passed through a 0.45 μm filter. The size of RG-I and pullulan particles was determined by a Malvern apparatus (ZetaSizer Nano) at 30 °C using a He–Ne laser, operating at 633 nm. Measurements were made by backscatter detection (the detector position at 173°). Analysis of measurement data was made using the Malvern DTS software, version 5.0. The DLS cumulant analysis was used to characterize samples through their mean hydrodynamic radius. Every radius value was an average of 10 measurements. Pullulans were used as standards to check the correlation of the self-diffusion coefficient (*D*) or hydrodynamic radius with the concentration of the polysaccharide solution.

2.8. NMR spectroscopy

The samples of RG-I and pullulans were dissolved in D_2O (99.9%, Ferak, Germany) to accomplish the H–D exchange of hydroxyl protons in polysaccharides and then, after drying, re-dissolved in

D_2O (99.994%, Aldrich, USA). All ^1H spectral, self-diffusion (Price, 2009), two-dimensional heteronuclear multiple bond correlation (HMBC) and rotating-frame nuclear Overhauser effect correlation spectroscopy (ROESY) experiments were conducted at 303 K using a Bruker AVANCE III NMR spectrometer operating at 600 MHz equipped with a standard *z*-gradient inverse probe head to produce gradients with the maximum field strength up to 55.7 G cm^{-1}. Diffusion experiments were performed using a stimulated-echo sequence incorporating bipolar gradient pulses and a longitudinal eddy current delay (BPP-LED) (Wu, Chen, & Johnson, 1995). The residual HOD signal was suppressed by means of presaturation. The gradient strength was varied from 2 to 95% of its maximum value over 64 increments for RG-I samples and 32 increments for pullulans under constant diffusion time (50 ms) and gradient pulse duration 20–30 ms for RG-I samples and 16–30 ms for pullulans. A recycle delay of 5 s was used to collect 8 transients in 32 k of data points. Data processing and analysis were performed using Topspin 2.1 software (Bruker, Germany). Two-dimensional homonuclear ROESY and heteronuclear HMBC experiments were recorded and processed using standard Bruker protocols.

3. Results

Hydrodynamic properties and spatial structure of RG-I from flax cell walls were characterized using SEC, DLS and NMR.

3.1. Chromatography

3.1.1. Initial RG-I

During gel-filtration on the Sepharose CL-4B column, the elution volume [$V_e(V_h)$] of RG-I corresponded to a broad region with a peak maximum (according to retention time of pullulan standards) in the region 200–400 kD (Fig. 1A). The molecular weight of RG-I calculated through the proportion of pores available for pullulan molecules (K_{av}) (Fig. 1B) was found to be in the range 50–1700 kD with a peak maximum at 240 kD. The weight-average ($\bar{M}_w$) and number-average ($\bar{M}_n$) molecular weights of RG-I, calculated by slice approach, were determined to be 367 kD and 221 kD, respectively. The polydispersity index equal to 1.7 was evidence of narrow molecular weight distribution of interpolymer in the RG-I composition.

3.1.2. Fragments of RG-I, obtained after galactanase treatment

Treatment of the cell wall RG-I of flax fibers with galactanase and chromatography of the obtained fragments on a Sepharose CL-4B column resulted in the separation of the low molecular weight fragments (G2) and the polymeric backbone (G1), which was observed in the same region as the initial polysaccharide (Fig. 1A). The fragments cleaved off by galactanase (G2) consisted mainly of galactose (99 mol%), with trace amounts of arabinose and glucose. Rhamnose was present only in the high molecular weight peak (G1), so the backbone was separated from the low molecular weight products of enzymatic degradation.

The Gal/Rha ratio decreased from 4.0 in the initial polymer to 1.6 in fraction G1. In total, around 45% of the sugars were removed from the polysaccharide by the galactanase, i.e. the molecular weight of RG-I was reduced by approximately half. However, the remaining polymeric part (fraction G1) eluted on the Sepharose CL-4B column at the same part of the profile as before treatment with the enzyme. In addition, after hydrolysis of RG-I by galactanase, the small peak appeared in the higher molecular weight region (Fig. 1A).

Molecular weight of G1 fraction of RG-I calculated through the proportion of pores available to the molecule (K_{av}) for pullulans (Fig. 1B), as well as for initial polymer, was in the range of 50–1700 kD with peak maximum value in region of 200–400 kD.

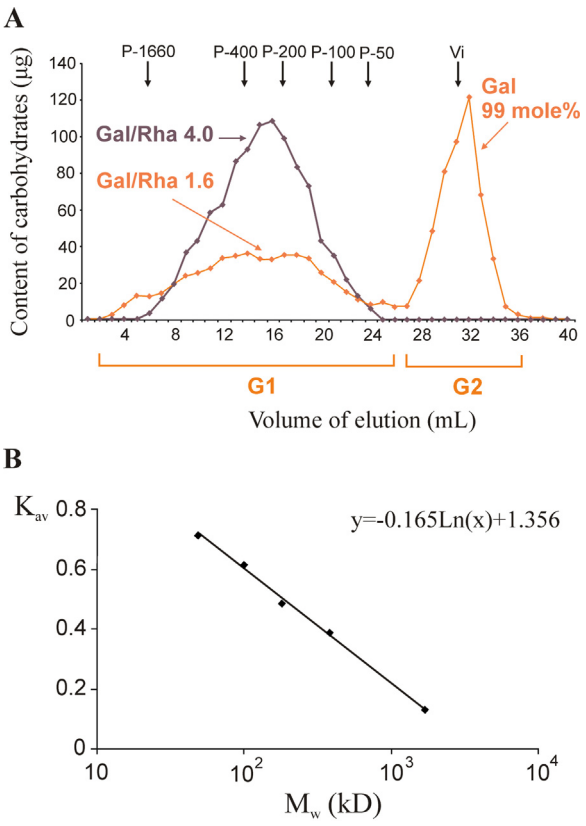

Fig. 1. Fractionation of the flax fiber cell wall RG-I (brown) and of its fragments obtained after hydrolysis by galactanase (orange) on a Sepharose CL-4B column (A). Pullulans were used as molecular weight markers. Selectivity plot of the Sepharose CL-4B for pullulans and relationship for molecular weight calculation through proportion of pores available to the molecule (K_{av}) (B). (For interpretation of the references to color in this figure legend, the reader is referred to the web version of this article.)

Calculated by slice approach weight-average ($\bar{M}_w$) and number-average ($\bar{M}_n$), the molecular weights of G1 fraction were 278 kD and 222 kD, respectively. The polydispersity index was 1.3. The molecular weight of G1, calculated via molecular weight of initial RG-I and monosaccharide compositions of RG-I and G1, was 213 kD.

Thus, the real molecular weight of the flax fiber RG-I did not correspond to the position of the peak on the size-exclusion chromatography profile.

3.2. Some β-(1 → 4)-galactose residues still remain attached to the backbone after galactanase treatment

Galactose residues were not completely removed from the backbone by the galactanase treatment: galactose remained among the main monosaccharides in the obtained polymeric fraction (41 mol%). Correspondingly, the major signals, which were present on ^1H NMR spectra of fraction G1 in the region 3.52–4.16 ppm, belong to galactose: H2, H3, H5, and H6 of galactose at 3.68–3.82 ppm, H1 (4.62 ppm), and H4 (4.16 ppm) of 1 → 4-linked galactose, and H4 of terminal galactose at 3.91 ppm (Fig. 2).

The proportion of non-branched and branched Rha residues, evaluated from the signal intensity of methyl group protons at 1.24 ppm and 1.31 ppm, respectively, as well as the proportion of side chains, presented by single galactose residues, evaluated from the signal intensity of H-2 (3.51 ppm), were not changed after hydrolysis of RG-I by galactanase (Fig. 2).

The Gal/Rha ratio in fraction G1 was low (1.6), but the oligomeric Gal chains were still present. The average length of oligomeric side

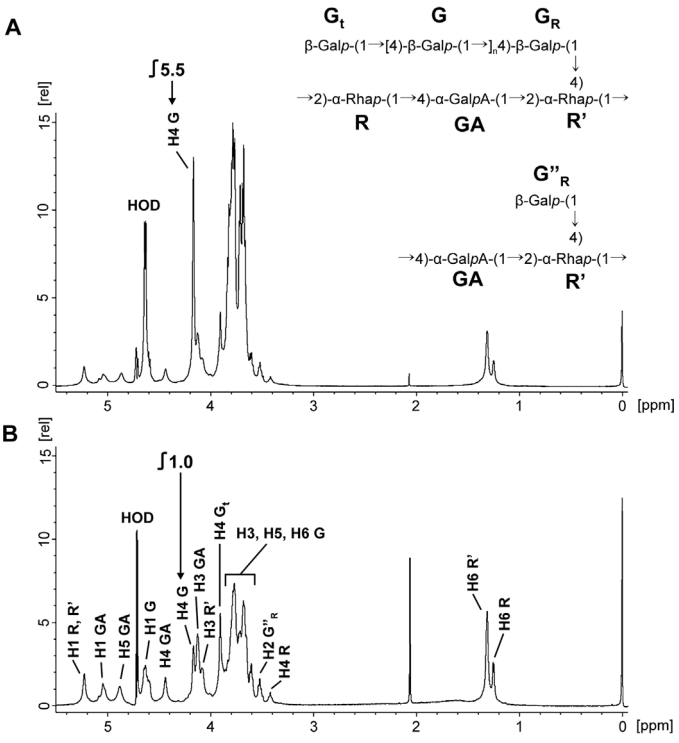

Fig. 2. ^{1}H NMR spectra of flax fiber cell wall RG-I (A) and its fragment G1 obtained after galactanase treatment and containing the whole backbone and residual side chains (B). Chemical shifts of ^{1}H were assigned according to Mikshina et al., 2012. The signal designations are presented in the scheme in the upper right part of the figure.

chains in fraction G1 accounted for 5–6 Gal residues. Signals at 4.16 ppm (Fig. 2) indicated that at least part of the oligomeric chains consisted of β-(1 → 4)-linked galactose, which was not totally removed from the backbone by the galactanase.

3.3. Diffusion experiments

To characterize the behavior of flax cell wall RG-I in solution and to establish the correlation between the hydrodynamic radius and molecular weight of this polysaccharide two techniques (DLS and NMR) with different principles of diffusion experiment were used. The advantage of DLS is the possibility to characterize both the hydrodynamic radius and molecular mass of particles. The advantage of the NMR experiment is the possibility to relate the self-diffusion coefficient to the certain spectral line in the ^{1}H NMR spectrum and to characterize both the mobility of the whole molecule and of its different structural elements. To verify the proposed approaches, pullulans of various molecular weights were used for determination of dependence between self-diffusion coefficient, hydrodynamic radius, and molecular weight of polymer. Basic molecular characteristics of pullulans in aqueous solutions were well-characterized earlier (Nishinari et al., 1991; Viel, Capitani, Mannina, & Serge, 2003).

3.3.1. Dynamic light scattering

Using the classical approach which applies the least-square fitting of the self-diffusion coefficient as a function of molecular weight in double-logarithmic coordinates for pullulans we got the equation $D = 8.1 \times 10^{-9} M_w^{-0.50}$ m^2 s^{-1}. The value of the exponent 0.50 is in good agreement with the described earlier conformation of pullulan in water as the flexible random coil (Kato, Katsuki, & Takahashi, 1984; Kawahara, Ohta, Miyamoto, & Nakamura, 1984; Nishinari et al., 1991). The exponent values for pullulans obtained by different methods varied from 0.49 to 0.55 (Kato et al., 1984; Nishinari et al., 1991; Viel et al., 2003). According to the Zimm model (Zimm, 1956; Doi & Edwards, 1988) an exponent values for flexible polymers are about 0.5 in a θ-solvent and 0.6 in a good solvent.

The self-diffusion coefficient of RG-I, calculated via Stokes–Einstein Eq. (2) using hydrodynamic radius (R_h) obtained in the DLS experiment, is depended on the concentration of polysaccharide in solution (Fig. 3A, data were taken from size distribution by number of particles).

$$D = \frac{kT}{6\pi\eta R_h}, \quad (2)$$

where D is the self-diffusion coefficient, k is Boltzmann's constant, T is the absolute temperature, η is solvent viscosity, and R_h is the hydrodynamic radius of the spherical particle.

We observed relatively constant values of the RG-I self-diffusion coefficient in concentrated solutions (0.8–5 mg mL^{-1}), followed by a sharp increase and then its retention at subsequent dilution (Fig. 3A). Hydrodynamic radii of RG-I particles for these two states were equal to 142–192 nm and 15–18 nm, correspondingly. The molecular weight of RG-I for the most diluted solutions calculated by the equation, obtained for pullulan standards, amounted to 140–210 kD. It is obvious that the dependence obtained for the linear pullulans cannot be directly used to calculate the molecular weight of RG-I, but these values can be compared with gel-filtration data (Fig. 1).

The shape of the self-diffusion coefficient concentration dependence for the fraction G1 obtained after RG-I hydrolysis by β-(1 → 4)-galactanase was similar to that of the initial polysaccharide (Fig. 3A) with plateau regions for concentrated (1.7–10 mg mL^{-1}) and diluted (0.1–0.8 mg mL^{-1}) systems with a sharp step between them. The hydrodynamic radius of particles in the G1 fraction for high concentration of polymer is approximately 14–26 nm corresponding to those for initial RG-I in more diluted solutions (Fig. 3A). The radius of particles at low concentrations of the G1 fraction decreased to approximately 2–2.5 nm, corresponding to a molecular weight 2.82 kD for infinite diluted solution according to the calibration equation obtained for pullulans.

3.3.2. NMR spectroscopy

The self-diffusion coefficient of pullulans was determined using different signals in the ^{1}H NMR spectrum of this polymer. The echo attenuation for pullulan samples was well described by one exponential component (Fig. 3B). The difference between self-diffusion coefficients obtained from different spectral lines in ^{1}H spectrum for every pullulan sample (P-50, P-100, P-400 and P-1600) did not exceed 2% (Fig. 3C). Hydrodynamic radii of pullulans obtained by NMR and DLS techniques (Table 1) were close to each other and corresponded to those reported previously (Viel et al., 2003). A least-square fitting of the self-diffusion data for pullulans yielded the dependence $D = 1.4 \times 10^{-8} M_w^{-0.56}$ m^2 s^{-1}.

Evaluating the value of chemical shift for each group of equivalent protons, we observed its approximately 0.025 ppm displacement to the weak field region for all signals at every step of dilution of the RG-I sample (Fig. 4). In the inverse coordinates ($d = f(1/C)$), the inflection point can be observed at a concentration of 8.3 mg mL^{-1}.

The diffusive decay for RG-I at different concentrations was non-exponential (Fig. 3B) which can result from either size distribution of particles or the character of their diffusion. To obtain from these curves the self-diffusion coefficient for RG-I particles we used the Kohlrausch–Williams–Watts function, circumscribing the fit of experimental data by a stretched exponent and taking

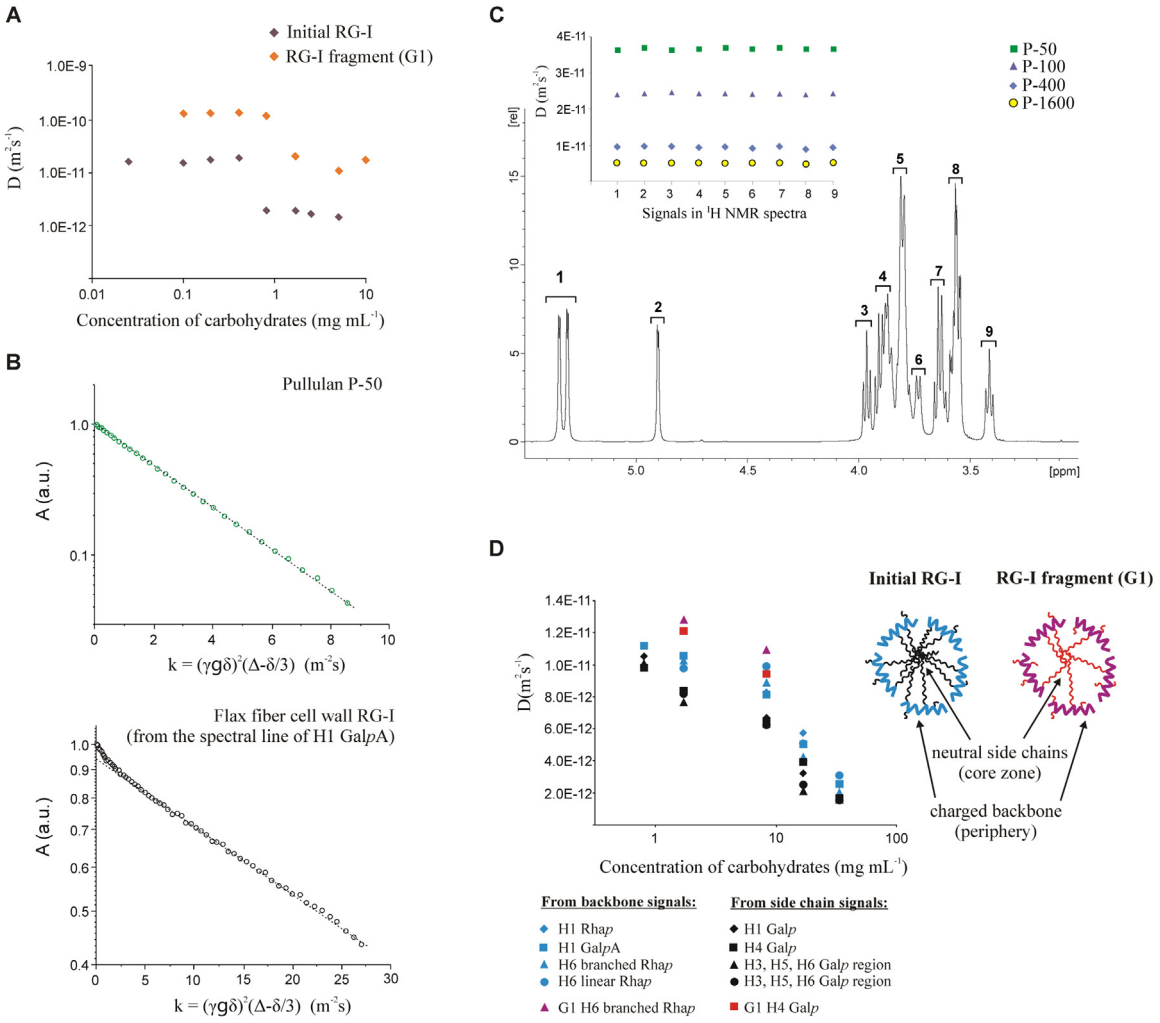

Fig. 3. Diffusion behavior of flax cell wall RG-I and pullulans in solution. (A) Dependence of self-diffusion coefficient determined by DLS on concentration of flax fiber cell wall RG-I (brown) and its fragment (G1) obtained after galactanase treatment and containing the whole backbone and residual side chains (orange). (B) Typical echo attenuation curves obtained for pullulan P-50 and for flax fiber cell wall RG-I. The latter is from the spectral line of H1 GalpA. (C) Typical ^{1}H NMR spectrum and self-diffusion coefficients of pullulans, determined using different signals (1–9) in ^{1}H NMR spectra. (D) Dependence of self-diffusion coefficient determined from different signals in the ^{1}H NMR spectrum on concentration of flax fiber cell wall RG-I and of its fragment (G1). A scheme of possible spatial structure of the initial polymer (blue/black) and fragment (G1) obtained after galactanase treatment and containing the whole backbone and residual side chains (purple/red). (For interpretation of the references to color in this figure legend, the reader is referred to the web version of this article.)

into account the factor of non-exponentiality β (Fleischer, Rittig, & Konak, 1998):

$$S_{\mathrm{inc}}(q,t) = \exp\left(-\left(q^2 tD\right)^{\beta}\right), \quad (3)$$

where S_{inc} is an incoherent scattering function, q is the generalized scattering vector with $|q| = \gamma\delta g$, γ is the gyromagnetic ratio of proton, δ is the gradient pulse duration, g is the amplitude of the field gradient pulse, t is the diffusion time, D is the self-diffusion coefficient, and β is the coefficient of non-exponentiality. In our experiments, the parameter β varied from 0.82 to 1.

Table 1
Self-diffusion coefficients and hydrodynamic radii (according to Stokes–Einstein equation) determined by DLS and NMR for pullulans (P), flax fiber cell wall RG-I and its fragment obtained after hydrolysis by galactanase (G1) in aqueous (H_2O, D_2O) solutions.

Sample	M_w (kD)	Dynamic light scattering		NMR spectroscopy	
		Self-diffusion coefficient, $\times 10^{-11}$ (m^2 s^{-1})	Hydrodynamic radius, nm	Self-diffusion coefficient, $\times 10^{-11}$ (m^2 s^{-1})	Hydrodynamic radius (nm)
P-1600	1 660[a]	0.64 ± 0.02	33.4	0.51 ± 0.01	34.7
P-400	380[a]	1.31 ± 0.01	16.3	0.95 ± 0.02	18.7
P-100	100[a]	2.75 ± 0.01	7.8	2.42 ± 0.02	7.3
P-50	48[a]	3.63 ± 0.02	5.9	3.67 ± 0.02	4.8
RG-I	50–1660[b]	1.57 ± 0.02[c]	17.7[c]	Two groups of signals, data	
G1	50–1660[b]	13.30 ± 0.12[c]	2.1[c]	presented in Fig. 3D	

[a] According to manufacturer information.
[b] According to gel-filtration.
[c] For infinite diluted solution.

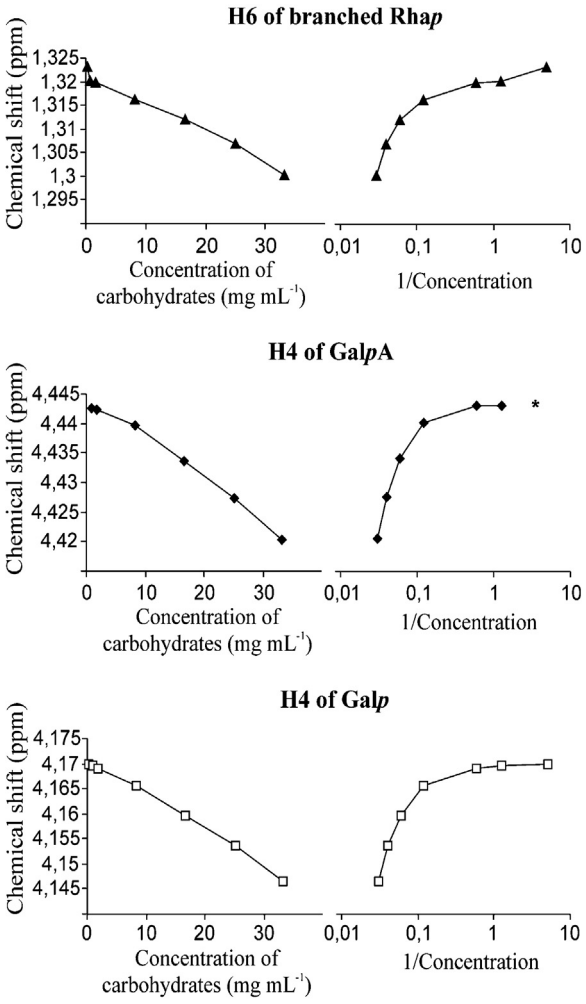

Fig. 4. Chemical shift changes for protons of backbone (methyl group of α-(1 → 2)-Rha*p* branched at O-4, H4 of [→4)-α-D-GalpA-(1→]) and side chains (β-(1 → 4)-Gal*p*) of flax fiber cell wall RG-I. *—low intensity signal.

To take into account non-exponential shape of diffusive decays (Fleischer et al., 1998) we calculated the average self-diffusion coefficients for RG-I samples (4) using the following equation:

$$\mathrm{Dav} = \frac{1}{\left\langle D^{-1} \right\rangle} = \frac{\beta D}{\Gamma\left(1/\beta\right)} \tag{4}$$

where Γ is the gamma-function, D is the self-diffusion coefficient, and β is the coefficient of non-exponentiality. These data are shown in Fig. 3D.

Self-diffusion coefficients of the RG-I backbone and side chain residues at various concentrations were determined only for the narrow weakly- or non-overlapping peaks of high intensity. Self-diffusion coefficients obtained using separate spectral lines of the RG-I spectrum differed. All self-diffusion coefficient data for RG-I could be divided into two distinct groups (Fig. 3D, black and blue markers). The first group (Fig. 3D, blue markers) was obtained from the signals of polymer backbone 5.23 ppm (H1), 1.31 ppm (H6) of branched rhamnose; 5.23 ppm (H1), 1.24 ppm (H6) of unbranched rhamnose, 5.03, and 5.05 ppm (H1) of galacturonic acid. The second group with lower values of self-diffusion coefficient (Fig. 3D, black markers) was obtained mainly from the signals of linear β-(1 → 4)-galactose, included 4.62 ppm (H1), 3.68 ppm (H2), 3.76 ppm (H3), 4.16 ppm (H4), 3.70 ppm (H5), 3.79, and 3.82 ppm (H6).

Upon dilution, the mobility of backbone and side chains of RG-I increased. At any concentration, the self-diffusion coefficients obtained from the rhamnose and galacturonic acid signals exceeded 1.2–1.5-fold the values obtained from galactose signals (Fig. 3D).

Self-diffusion coefficient for the fraction G1 obtained after RG-I hydrolysis by β-(1 → 4)-galactanase could be well determined by BPP-LED only for the spectral lines of methyl protons of rhamnose and H4 galactose, and only for high concentrated samples (1.7–8.3 mg mL^{-1}) (Fig. 3D, purple and red markers). In dilute solutions, the intensity of signals was very low. After the treatment of RG-I by galactanase, the self-diffusion coefficient, obtained for analyzed signals of the G1 fraction, increased approximately 1.4-fold in comparison with the initial RG-I at the same concentrations. These values were very similar to those obtained by DLS. The self-diffusion coefficient obtained from spectral lines of methyl protons of rhamnose exceeded the self-diffusion coefficient obtained from spectral lines of galactose by 1.1–1.2-fold.

Thus, the diffusion experiments demonstrated that the mobility of initial flax RG-I increased at dilutions approximately 10-fold within the observable concentration range (Fig. 3A and D). The molecular weight of RG-I determined for diluted solutions by DLS and NMR techniques using a calibration curve for pullulans corresponded to that observed by gel-filtration (~200 kD). NMR experiments demonstrated that the backbone of flax RG-I had higher mobility than the side chains. The mobility of RG-I fragments (G1), which was observed at the same elution volume as the initial RG-I despite the removal of a considerable number of galactose side chains, was at high concentrations similar to more diluted solutions of initial RG-I. The mobility of these fragments dramatically increased at dilution corresponding, if applied to pullulans, to a molecular weight decrease from ~200 kD to ~3 kD.

3.4. Galactose side chains are attached to RG-I backbone

The difference in the mobility of the RG-I side chains and backbone could be caused by the absence of a chemical bond between them. To prove that the galactose side chains were indeed attached to the backbone, we used HMBC experiments, which allows the estimation of the long-range coupled ^{1}H and ^{13}C (J_{CH} < 10 Hz), and ROESY, which demonstrates the spatial proximity of protons.

The inter-residue cross-peak at δ 4.62/82.2 in the HMBC spectrum (Fig. 5), assigned to the Gal H1/Rha C4 correlation, confirmed the presence of linkages between galactose and rhamnose residues. The intensive cross-peak at δ 4.62/79.4 indicated that the 1 position of Gal*p* residues was linked to the 4 position of Gal*p* residues by 1 → 4 glycosidic linkage. Others cross-peaks on the fragment of the RG-I HMBC spectrum were mainly assigned to correlations of H1 with C2, C3, and C5 of galactose residues.

In the fragment of the RG-I ROESY spectrum, the H1 of Gal*p* (4.62 ppm) correlated with the methyl protons of the branched rhamnose (1.31 ppm) (Fig. 5), which also could be evidence for the linkage between galactose side chains and the backbone of RG-I.

4. Discussion

Characterization of physicochemical properties and spatial structure of non-linear polysaccharides is a serious challenge. This primarily is due to their high molecular weight and structure complexity. Besides, the structure of polysaccharides is not directly encoded in the genome, and there is some variability in many parameters of these polymers (such as molecular weight, length, and location of the side chains, and the presence of the modifying groups). This significantly complicates the analysis of heteropolysaccharides, especially those that are as complex as RGs-I. As a consequence, studies devoted to the characterization of hydrodynamic behavior of RG-I are scarce (Sengkhamparn et al.,

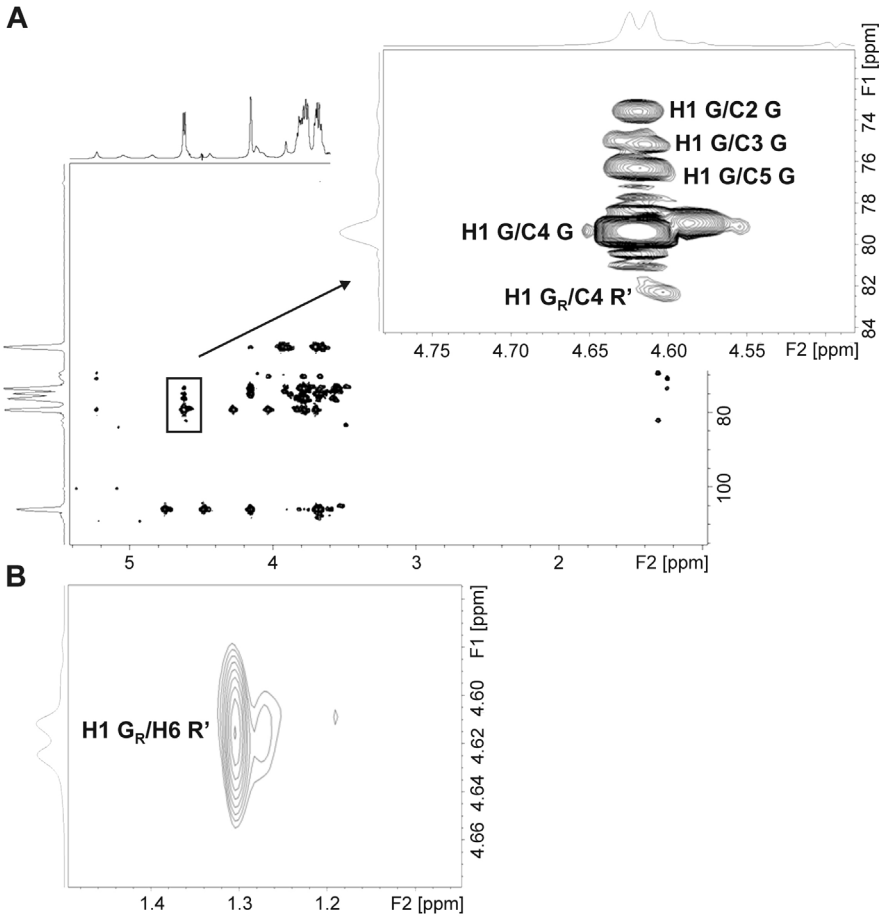

Fig. 5. Fragments of HMBC (A) and ROESY (B) spectra of flax fiber cell wall RG-I. The signal designations are presented in Fig. 2.

2010; Kontogiorgos, Margelou, Georgiadis, & Ritzoulis, 2010). The present study considers the physicochemical properties of RG-I from the flax gelatinous cell wall and demonstrates that combination of complementary diffusion techniques provides information on the possible organization of complex heteropolysaccharides, such as RG-I.

4.1. Flax fiber cell wall RG-I retains hydrodynamic volume after galactanase treatment

Chromatographic analysis of RG-I fragments, obtained after galactanase treatment, revealed that the whole polymer backbone with residual side chains (faction G1) eluted on the Sepharose CL-4B column at the same part of profile, though around half of the carbohydrates were removed. It is known that the separation of polymers using size-exclusion chromatography is based on their hydrodynamic volume rather than molecular weight (Grubisic, Rempp, & Benoit, 1967). Thus, the flax cell wall RG-I retains hydrodynamic volume after the removal of a considerable portion of its galactose side chains.

4.2. Side chains of flax fiber RG-I have lower mobility than the backbone

According to BPP-LED experiments, the backbone of RG-I is more mobile than the side chains. The difference in the values of self-diffusion coefficient is present at all concentrations studied and constitutes the 1.3–1.9-fold. These values are quite significant since they are comparable to the difference in mobility between two pullulans with molecular weight 100 and 48 kD (~1.5 times) (Fig. 3C) or 270 and 670 kD (~1.5 times) (Viel et al., 2003). The reason of this difference in mobility is not the absence of linkage between the RG-I backbone and the galactan chains: NMR data obtained in this study give the direct evidence of a covalent bond between galactan and RG-I (Fig. 5). Besides, the evidence of linkage between galactan chains and the RG-I backbone in the polymer from the flax fiber is provided by the formation of $(Rha\text{-}GalA)_nGal_m$ oligosaccharides after RG-I backbone hydrolysis by RG hydrolase (Mikshina et al., 2012; Gur'janov et al., 2007). This is also in agreement with the general consideration of higher plant β-(1 → 4)-galactan as a side chain of RG-I (McCann & Roberts, 1991; Carpita & Gibeaut, 1993; Ridley et al., 2001; Caffal & Mohnen, 2009).

The observed reduction in the side chain mobility for complex RG-I from flax fiber cell wall can originate from interaction of side chains with each other. Indirect evidence in favor of this idea is the more pronounced difference in the mobility of the RG-I backbone and side chains in concentrated solutions (8.3–33.3 mg mL^{-1}). After the hydrolysis of RG-I by galactanase, the backbone is still more mobile compared to the side chains, but the difference in mobility of these structural elements in the G1 fraction becomes smaller than in the initial RG-I at the same solution concentrations.

Dilution of the RG-I and G1 fraction solutions leads to ~10 times reduction in the particle size (Fig. 3A). In the absence of molecular association, such a transition cannot occur without breaking of glycosidic bonds. The glycoside bond breakage simply at the dilution of solution is not possible. Thus, the above data suggest the association of RG-I molecules in solution. The higher mobility of the backbone in comparison to the side chains can be related to its location at the periphery of the RG-I molecule associate (Fig. 3D). The removal of considerable portion of the side chains by galactanase, while still

leaving some of them, permitted to hold together the associate, and consequently, to keep hydrodynamic volume at gel-filtration.

4.3. Three conjectured levels of interaction of flax RG-I molecules in solution

The step-wise drop in mobility with the increase in concentration was revealed in the DLS experiments for the initial RG-I and for the G1 fraction (Fig. 3A). Such behavior in solution can be ascribed to the aggregation of polysaccharide molecules (Sengkhamparn et al., 2010). The changes of chemical shifts observed by NMR at the dilution of RG-I samples (Fig. 4) can also take place because of association of its molecules.

Three levels of molecule organization can be suggested basing on the results of DLS analysis of RG-I and G1 (Fig. 3A). The first level ("elementary unit") is observed for fragments of the G1 fraction at dilution of sample. The hydrodynamic radius of such units is 2–2.5 nm. They appear only when a considerable portion of the galactose side chains has been removed by galactanase. The second level ("associate of elementary units") includes the G1 fraction at high concentrations and the initial RG-I in dilute solutions. The hydrodynamic radius of these structures is 15–20 nm. This level of RG-I and G1 organization probably corresponds to the molecule state observed in size-exclusion chromatography. The third level is the "aggregates of associates" ("bunch of grapes"); it is observed for only initial RG-I in high-concentrated solutions. The size of these aggregates reaches 150–200 nm.

4.4. The nature of interactions between flax fiber RG-I molecules to form associates

The peculiar spatial structure of flax fiber RG-I molecules is related to galactose side chains, since their partial removal (G1) leads to the disruption of associates into "elementary units" in diluted solutions, while the associates of initial RG-I do not fall apart at the same concentrations. Aggregates of associates (150–200 nm) are not formed after RG-I hydrolysis by galactanase. This also suggests the participation of galactose side chains in aggregation. The sophisticated structure of RG-I side chains from flax fiber cell wall (Gurjanov et al., 2008; Mikshina et al., 2012) distinguishes this polysaccharide from pectins obtained from other plant sources.

Two types of RG-I molecular interactions have been suggested earlier. Based on DLS comparison of saponified and non-saponified okra RG-I, the hydrophobic interactions due to acetyl groups were demonstrated to be the reason for aggregation (Sengkhamparn et al., 2010). Mainly, these interactions are caused by acetylated galacturonic acid residues, but also it was found that acetylation of rhamnose residues at O-3 plays a key role in the association of okra RG-I molecules. Another type of RG-I-based supramolecular structure was suggested, rather speculatively, for RG-I isolated from sugar beet–covalent cross-linking of the arabinan side chains via dehydrodiferulates (Morris, Ralet, Bonnin, Thibault, & Harding, 2010).

RG-I from the gelatinous flax fibers is obtained after concentrated alkali treatment of cell wall and subsequent cellulose degradation. Thus, the acetyl groups in this polysaccharide are absent as is confirmed by NMR study (Fig. 2). Arabinan side chains and ferulates are not present. Prolonged regions of polygalacturonic acid, which can lead to different types of interactions in combined PGA + RG-I pectin molecules from other plant sources, are not detected in flax fiber polysaccharide. In particular, this is confirmed by the absence of the signals assigned to the [→4)-α-Gal*p*A-(1 → 4)-α-Gal*p*A-(1→] fragment in the HSQC spectrum of RG-I from the cell wall of flax fibers (data not shown) and by equal proportions of Rha and GalA obtained in monosaccharide analysis (Mikshina et al., 2012).

In this situation, keeping in mind that the non-covalent interactions of side chains made from β-(1 → 4)-galactan are important, hydrogen bonds seem to be the most obvious type of galactose chain interaction. However, the treatment of RG-I sample with activated by LiCl dimethylacetamide or with concentrated alkali does not lead to the formation of low molecular weight fragments (Gurjanov et al., 2008). Another possible explanation for associate maintenance with the involvement of galactan chains can be their mechanical entangling. Part of this entangling could be from the β-(1 → 4)-galactan secondary structure, which is characterized as a hollow helix (Fukushima, Tanaka, Azuma, & Iwata, 1997; Cid et al., 2010). Such structures may form coaxial helixes (reviewed by Gorshkova, Kozlova, & Mikshina, 2013). Besides, it was demonstrated that neutral side chains of RG-I could be implicated in the water binding capacity (Ulvskov et al., 2005). In our experiments, the level of association depends on sample dilution, indicating that water molecules could play an important role during associate formation. It is interesting to note that the very stable complexes of flax RG-I-derived oligosaccharides with water are detected by mass-spectrometry (Mikshina et al., 2012). The formation of these complexes is observed only for oligosaccharides with DP > 4.

Thus, the most probable explanation of the nature of unusual behavior of flax cell wall RG-I at gel-filtration can be the particular spatial organization of this polysaccharide. Such organization can be realized due to molecule association, which is formed by interacting side chains (core zone) and with backbone disposed at the surface of the associate (Fig. 3D). This type of associate is the newly described one; its characterization was made possible by the combination of two techniques, DLS and NMR, for diffusion experiments. Such spatial organization fits the idea of the RG-I function in G-layer as the causative agent for cellulose microfibril tension (Mikshina et al., 2013).

5. Conclusions

In this study, we have shown that combination of complementary diffusion techniques can provide information on the possible organization of complex heteropolysaccharides, such as RG-I. It was established that flax fiber RG-I retains the elution volume after enzymatic removal of considerable portion of the galactose side chains, leading to decrease in molecular weight by approximately half of the initial value. Different diffusion approaches suggest that this property can be related to the spatial organization of the polysaccharide and to the newly described capability of its molecules to form aggregates with the backbone located at the periphery.

Acknowledgments

This work was partially supported by grants from the Russian Foundation for Basic Research (projects 11-04-01602, 12-04-97077 and 14-04-31462). We thank Prof. Henk A. Schols (Wageningen University, the Netherlands) and Dr. Claudine Morvan (University of Rouen, France) for providing highly purified enzymes, Dr. Boris N. Khlebtsov (Institute of Biochemistry and Physiology of Plants and Microorganisms RAS, Russia) and Prof. Ivan I. Stoikov (Kazan (Volga Region) Federal University, Russia) for consultation and technical support at DLS experiments.

References

Bowling, A. J., & Vaughn, K. C. (2008). Immunocytochemical characterization of tension wood: Gelatinous fibers contain more than just cellulose. *American Journal of Botany*, *95*, 655–663.

Bradford, M. M. (1976). A rapid and sensitive method for quantitation of microgram quantities of protein utilizing the principle of protein–dye-binding. *Analytical Biochemistry*, *72*, 248–254.

Caffall, K. H., & Mohnen, D. (2009). The structure, function and biosynthesis of pectic polysaccharides in the context of the whole plant cell wall. *Carbohydrate Research*, *344*, 1879–1900.

Carpita, N. C., & Gibeaut, D. M. (1993). Structural models of primary cell walls in flowering plants: Consistency of molecular structure with the physical properties of the walls during growth. *Plant Journal*, *3*, 1–30.

Cid, M., Pedersen, H. L., Kaneko, S., Coutinho, P. M., Henrissat, B., Willats, W. G. T., et al. (2010). Recognition of the helical structure of β-1,4-galactan by a new family of carbohydrate-binding modules. *Journal of Biological Chemistry*, *285*, 35999–36009.

Doi, M., & Edwards, S. F. (1988). *The theory of polymer dynamics*. Oxford: Oxford University Press.

Dubois, M., Gilles, K. A., & Hamilton, J. K. (1956). Colorimetric method for determination of sugars and related substances. *Analytical Chemistry*, *28*, 350–356.

Fleischer, G., Rittig, F., & Konak, C. J. (1998). Influence of associations on self-diffusion of styrene–methylmethacrylate random copolymers in semidilute acetone solution. *Polymer Science, B: Polymer Physics*, *36*, 2931–2939.

Fukushima, A., Tanaka, F., Azuma, J., & Iwata, T. (1997). Characterization of β-(1 → 4)-D-galactan. *Wood Research*, *84*, 37–38.

Gorshkova, T., & Morvan, C. (2006). Secondary cell-wall assembly in flax phloem fibres: Role of galactans. *Planta*, *223*, 149–158.

Gorshkova, T. A., Chemikosova, S. B., Salnikov, V. V., Pavlencheva, N. V., Gurjanov, O. P., Stoll-Smits, T., et al. (2004). Occurrence of cell-specific galactan is coinciding with bast fibre developmental transition in flax. *Industrial Crops and Products*, *19*, 217–224.

Gorshkova, T. A., Gurjanov, O. P., Mikshina, P. V., Ibragimova, N. N., Mokshina, N. E., Salnikov, V. V., et al. (2010). A special type of secondary cell wall, formed by plant fibers. *Russian Journal of Plant Physiology*, *57*, 346–361.

Gorshkova, T. A., Kozlova, L. V., & Mikshina, P. V. (2013). Spatial structure of plant cell wall polysaccharides and its functional significance. *Biochemistry (Moscow)*, *78*, 836–853.

Grubisic, Z., Rempp, P., & Benoit, H. (1967). A universal calibration for gel permeation chromatography. *Journal of Polymer Science, B*, *5*, 753–759.

Gur'janov, O. P., Gorshkova, T. A., Kabel, M. A., Schols, H. A., & van Dam, J. E. G. (2007). MALDI-TOF MS evidence for the linking of flax bast fibre galactan to rhamnogalacturonan backbone. *Carbohydrate Polymers*, *67*, 86–96.

Gurjanov, O. P., Ibragimova, N. N., Gnezdilov, O. I., & Gorshkova, T. A. (2008). Polysaccharides, tightly bound to cellulose in the cell wall of flax bast fibre: Isolation and identification. *Carbohydrate Research*, *72*, 719–729.

Kato, T., Katsuki, T., & Takahashi, A. (1984). Static and dynamic solution properties of pullulan in a dilute solution. *Macromolecules*, *17*, 1726–1730.

Kawahara, K., Ohta, K., Miyamoto, H., & Nakamura, S. (1984). Preparation and solution properties of pullulan fractions as standard samples for water-soluble polymers. *Carbohydrate Polymers*, *4*, 335–356.

Kontogiorgos, V., Margelou, I., Georgiadis, N., & Ritzoulis, C. (2010). Rheological characterization of okra pectins. *Food Hydrocolloids*, *29*, 356–362.

McCann, M. C., & Roberts, K. (1991). Architecture of the primary cell wall. In C. W. Lloyd (Ed.), *The cytoskeletal basis of plant growth and form* (pp. 109–129). London: Academic Press.

McNeil, M., Darvill, A. G., & Albersheim, P. (1980). Structure of plant cell walls X. Rhamnogalacturonan I, a structurally complex pectic polysaccharide in the walls of suspension-cultured sycamore cells. *Plant Physiology*, *66*, 1128–1134.

Mellerowicz, E. J., & Gorshkova, T. A. (2012). Tensional stress generation in gelatinous fibres: A review and possible mechanism based on cell-wall structure and composition. *Journal of Experimental Botany*, *63*, 551–565.

Mellerowicz, E. J., Immerzeel, P., & Hayashi, T. (2008). Xyloglucan: The molecular muscle of trees. *Annals of Botany*, *102*, 659–665.

Mikshina, P. V., Gur'janov, O. P., Mukhitova, F. K., Petrova, A. A., Shashkov, A. S., & Gorshkova, T. A. (2012). Structural details of pectic galactan from the secondary cell walls of flax *(Linum usitatissimum* L.) phloem fibres. *Carbohydrate Polymers*, *87*, 853–861.

Mikshina, P. V., Chernova, T. E., Chemikosova, S. B., Ibragimova, N. N., Mokshina, N. Y., & Gorshkova, T. A. (2013). Cellulosic fibers: Role of matrix polysaccharides in structure and function. In T. van de Ven, & L. Godbout (Eds.), *Cellulose—fundamental aspects* (pp. 91–113). Rijeka: InTech.

Morris, G. A., Ralet, M. C., Bonnin, E., Thibault, J. F., & Harding, S. E. (2010). Physical characterisation of the rhamnogalacturonan and homogalacturonan fractions of sugar beet (*Beta vulgaris*) pectin. *Carbohydrate Polymers*, *82*, 1161–1167.

Nishinari, K., Kohyama, K., Williams, P. A., Phillips, G. O., Burchard, W. D., & Ogino, K. (1991). Solution properties of pullulans. *Macromolecules*, *24*, 5590–5593.

Price, W. S. (2009). *NMR studies of translational motion*. Cambridge: Cambridge University Press.

Ridley, B. L., O'Neill, M. A., & Mohnen, D. (2001). Pectins: Structure, biosynthesis, and oligogalacturonide-related signaling. *Phytochemistry*, *57*, 929–967.

Sengkhamparn, N., Sagis, L. M. C., Vries, R., Schols, H. A., Sajjaanantakul, T., & Voragen, A. G. J. (2010). Physicochemcial properties of pectins from Okra (*Abelmoschus esculentus* (L.) Moench). *Food Hydrocolloids*, *24*, 35–41.

Ulvskov, P., Wium, H., Bruce, D., Jørgensen, B., Qvist, K. B., Skjøt, M., et al. (2005). Biophysical consequences of remodeling the neutral side chains of rhamnogalacturonan I in tubers of transgenic potatoes. *Planta*, *220*, 609–620.

Van de Vis, J. W., Searle-van Leeuwen, M. J. F., Siliha, H. A., Kormelink, F. J. M., & Voragen, A. G. J. (1991). Purification and characterization of endo-1,4-β-d-galactanases from *Aspergillus niger* and *Aspergillus aculeatus*: Use in combination with arabinanases from *Aspergillus niger* in enzymic conversion of potato arabinogalactan. *Carbohydrate Polymers*, *16*, 167–187.

Viel, S., Capitani, D., Mannina, L., & Serge, A. (2003). Diffusion-ordered NMR spectroscopy: A versatile tool for the molecular weight determination of uncharged polysaccharides. *Biomacromolecules*, *4*, 1843–1847.

Visser, J., & Voragen, A. G. J. (1996). *Pectins and pectinases. Progress in biotechnology* (Vol. 14) Amsterdam: Elsevier.

Wu, D., Chen, A., & Johnson, C. S., Jr. (1995). An improved diffusion-ordered spectroscopy experiment incorporating bipolar gradient pulses. *Journal of Magnetic Resonance, Series A*, *115*, 260–264.

Yapo, B. M. (2011). Rhamnogalacturonan-I: A structurally puzzling and functionally versatile polysaccharide from plant cell walls and mucilages. *Polymer Review*, *51*, 391–413.

Zimm, B. H. J. (1956). Dynamics of polymer molecules in dilute solution: Viscoelasticity, flow birefringence and dielectric loss. *Chemical Physics*, *24*, 269–278.